Author(s): Lashab, M., Hraga, H. I., Abd-Alhameed, Raed A., Zebiri, C., Benabdelaziz, F. and Jones, S. M. R.

Title: Horn Antennas Loaded with Metamaterial for UWB Applications.
Publication year: 2011

Conference title: Progress In Electromagnetics Research Symposium Proceedings, Marrakesh, Morocco, March 20-23, 2011.

Publisher: The Electromagnetics Academy.

Link to original published version:
http://www.piers.org/piersproceedings/piers2011MarrakeshProc.php

Citation: Lashab, M., Hraga, H. I., Abd-Alhameed, Raed A., Zebiri, C., Benabdelaziz, F. and Jones, S. M. R. (2011). Horn Antennas Loaded with Metamaterial for UWB Applications. In: Progress In Electromagnetics Research Symposium Proceedings, Marrakesh, Morocco, March 20-23, 2011. Cambridge, MA: The Electromagnetics Academy, pp.1052-1065.

Horn Antennas Loaded with Metamaterial for UWB Applications

M. Lashab[1], **H. I. Hraga**[2], **Read Abd-Alhameed**[2], **C. Zebiri**[1], **F. Benabdelaziz**[1], **and S. M. R. Jones**[2]

[1]Electronics Department, Skikda University, Algeria
[2]Mobile and Satellite Communication Research Centre, University of Bradford, Bradford, UK

Abstract— In this paper, a conical horn antenna has been designed for Ultra-Wideband applications by loading its section with a metamaterial. The work aims first to compare results obtained by the wavelet-moment method to a simulation performed using HFSS. Secondly the conical horn is loaded with a very thin layer of metamaterial to enhance the radiation pattern and the bandwidth performance of the conical horn antenna and reduce the size of the antenna. The operating bandwidth of the proposed antenna is in the range of 10–13 GHz. The results obtained from HFSS and moment method are in good agreement.

1. INTRODUCTION

Artificial materials such as metamaterials and chiral media have recently been of great interest, both theoretically [1, 2], and experimentally [3, 4]. Metamaterials, for instance, exhibit either negative permittivity or negative permeability. If both of them are negative at a given frequency, the material is characterised by an effective negative index of refraction, so it is often referred to as a left handed metamaterial (LHMs). This type has interested many researchers, e.g., [5, 6]. The main objective of research on LHMs is improvement of the radiation pattern, directivity and bandwidth, and antenna size reduction. However in this paper a low index of permittivity is used to characterize the metamaterial as introduced by [7].

Horn antennas loaded with dielectrics or ferrite materials [8], have desirable properties such as increased directivity, reduced side lobe level, wide bandwidth, low loss, and ease of fabrication [9, 12]. These properties are particularly attractive for applications such as ultra-wideband (UWB) ground penetrating radars (GPR) [13, 14]. However, the characterization of such antennas with increasingly complex designs using analytical techniques is often not possible. On the other hand, a numerical model can provide a virtual test bench to explore different design possibilities before any costly prototyping. Although many numerical techniques can be used to model and study the characteristics of such antennas, the moment method is well known to provide good accuracy [15, 16]. In this paper, an improvement has been made by the introduction of wavelets.

This paper deals firstly with a comparison between an improved moment method and Ansoft's HFSS, then an observation is made of the effect of loading the horn antenna.

2. FORMULATION

2.1. Moment Method Formulation

2.1.1. Integral Equation

The Conical Horn is studied in 3D as shown in Figure 1, the construction of this horn is considered to be from any type of material. Using the boundary conditions, the scattered field may be written as an integral magnetic equation in two dimensions for a PEC structure as:

$$K(J(r)) = \frac{1}{2}J(r) - \hat{n} \times \int_S J(r') \times \nabla' G(r, r') \cdot ds' = \hat{n} \times H^i(r) \tag{1}$$

Here $G(r, r')$ is Green's function and $J(r)$ is the current density, this can be expressed in terms of the tangential components. Because the antenna is a body of revolution, the current may be expanded as follow:

$$\vec{J}(t, \varphi) = \sum_{\nu=-\infty}^{+\infty} \left[J_t(t, \varphi) \cdot \hat{t} + J_\varphi(t, \varphi) \cdot \hat{\varphi}\right] \cdot e^{j\nu \cdot \varphi} \tag{2}$$

where $(J_t,\ J_\varphi)$ are the tangential components of the current on the surface of the antenna.

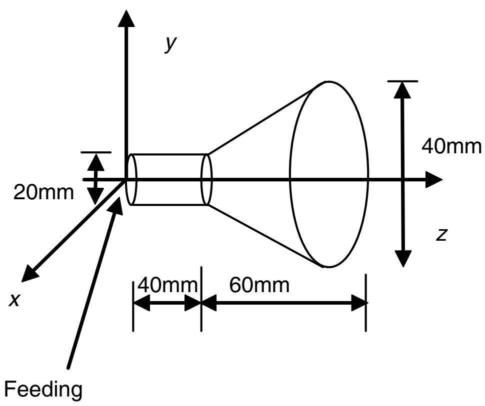

Figure 1: Conical horn in 3D.

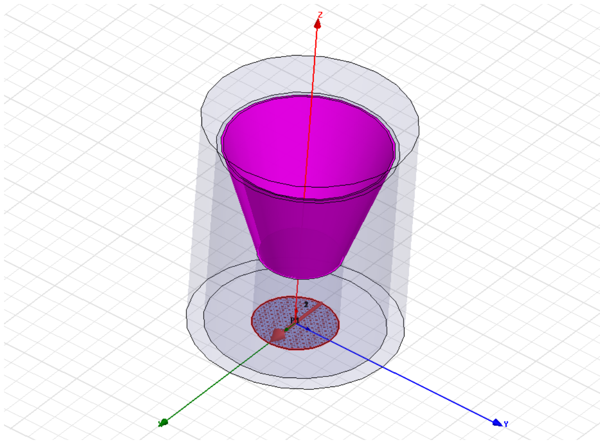

Figure 2: Horn antenna designed by HFSS.

2.1.2. Moment Method

The Moment method is applied on the integral Equation (1), this is discritised by using sets of basis and testing functions [13].

Let W and J denote testing and basis functions, respectively. The integral equation is projected over the two tangential components using the expansion (2). This is done by applying the inner product, denoted by the bracket in (3), to yield:

$$\left\langle \vec{W}, K(J(r)) \right\rangle = \left\langle \vec{W}, \hat{n} \times H^{i}(r) \right\rangle \tag{3}$$

2.2. Wavelets Expansion

2.2.1. Basis Functions

The basis and testing functions are presented as a superposition of wavelets at several scales and include a scaling function. A Galerkin's method is then applied to transform the integral equation into algebraic equations in the expansion coefficients.

2.2.2. Wavelets Application

The wavelets are applied directly to the integral equation. The current density is expanded as follows

$$J_t(t,\varphi) = \sum_{n=0}^{2^0-1} a_n^t \cdot \phi_{j,n}^t(t,\varphi) + \sum_{m=0}^{j} \sum_{n=0}^{2^{m-1}} c_{m,n}^t \psi_{m,n}^t(t,\varphi) \tag{4}$$

$$J_\varphi(t,\varphi) = \sum_{n=0}^{2^0-1} a_n^\varphi \cdot \phi_{j,n}^\varphi(t,\varphi) + \sum_{m=0}^{j} \sum_{n=0}^{2^{m-1}} c_{m,n}^\varphi \psi_{m,n}^\varphi(t,\varphi) \tag{5}$$

Here $(\psi_{m,n}^t, \psi_{m,n}^\varphi)$ and $(\phi_{j,n}^t, \phi_{j,n}^\varphi)$ are the mother and the scaling wavelets, respectively. The corresponding expansion coefficients are a_m^t, $c_{m,n}^t$ and a_n^φ, $c_{m,n}^\varphi$. Using equations (4) and (5) in (3), the following matrix equation is obtained:

$$\begin{bmatrix} Z_{m,n}^{tt} & Z_{m,n}^{t\varphi} \\ Z_{m,n}^{\varphi \cdot t} & Z_{m,n}^{\varphi\varphi} \end{bmatrix} \cdot \begin{bmatrix} c_{m,n}^t \\ c_{m,n}^\varphi \end{bmatrix} = \begin{bmatrix} H_1 \\ H_2 \end{bmatrix} \tag{6}$$

The terms a_m^t, a_n^φ are considered very small, thereby they are neglected. The matrix elements are expressed as follow:

$$Z_{pq}^{tt} = \int_t \frac{1}{2} \cdot W_q^t J_p^t \rho \cdot dt - \int_t \int_{t'} W_q^t J_p^t \cdot \hat{\varphi} \times \hat{t}' \cdot I_G \cdot \rho \rho' dt' dt \tag{6a}$$

Here, $I_G = \int_0^{2\pi} \nabla G(r, r') \cdot e^{jv \cdot \varphi'} d\varphi'$.

In more detail, this is given as an integral over the interval $[0, 1]$:

$$Z_{pq}^{tt} = \left\langle \psi_p, \left\langle \psi_q, \frac{1}{2} - T(t,t) \cdot \Omega(t,\xi) \right\rangle \right\rangle \tag{7}$$

where $T(t,t)$ is the term under the double integral of the second part of Equation (6a). In the same manner the other components are given.

$$Z_{pq}^{\varphi\varphi} = \left\langle \psi_p, \left\langle \psi_q, \frac{1}{2} + T(\varphi,\varphi) \cdot \Omega(t,\xi) \right\rangle \right\rangle \tag{8}$$

$$Z_{pq}^{\varphi \cdot t} = \langle \psi_q, \langle \psi_p, T(\varphi,t) \cdot \Omega(t,\xi) \rangle \rangle \tag{9}$$

$$Z_{pq}^{t\varphi} = -\langle \psi_q, \langle \psi_p, T(t,\varphi) \cdot \Omega(t,\xi) \rangle \rangle \tag{10}$$

where $\Omega(t,\varphi,\xi)$ is the calibration of the changing variables, and $D(\xi) = |dt/d\xi|$. The other elements can be written in the same manner. Similarly for the excitation the matrix elements are also expressed as an inner product by:

$$H_1 = \left\langle \psi_q, H^t I_{G2} \cdot \Omega(t,\xi) \right\rangle \tag{11}$$

$$H_2 = -\langle \psi_q, H^\varphi I_{G2} \cdot \Omega(t,\xi) \rangle \tag{12}$$

where $I_{G2} = \frac{1}{2\pi} \int_0^{2\pi} e^{-jv\cdot\varphi} d\varphi$.

The unknowns $[c_{m,n}^t, c_{m,n}^\varphi]$ should be calculated from Equation (6). The current density and the radiation pattern may then be obtained.

3. NUMERICAL RESULTS

In the moment method, the wavelet employed is constructed from the Haar orthogonal wavelet with vanishing moment $N = 7$, the lowest resolution level is chosen Since 128 wavelets are involved, a system of matrices (of 128×128 elements) is generated.

The surface of the taper of the horn is a metamaterial, considered to be an isotropic low index type, in a very thin layer of 1 mm thickness. The permittivity and permeability are respectively $\varepsilon_r = 0.5$, $\mu = 1$. The horn loaded with metamaterial as designed by HFSS is shown in Figure 2. The results obtained by the wavelet-based moment method are in good agreement with the results obtained by HFSS in all the figures of the radiation pattern except the reflection coefficient figure.

The radiation pattern in H-Plane given in Figure 3 and E-Plane in Figure 4 show a slight reduction of the side lobe in the H-plane, and almost no change in the E-plane. A very remarkable reduction in the cross polarization in Figure 5, this is more then 20% of reduction in the side lobes. The directivity and the gain are presented in Figure 6 and Figure 7, the antenna is more directive and better gain when loaded with metamaterial than without.

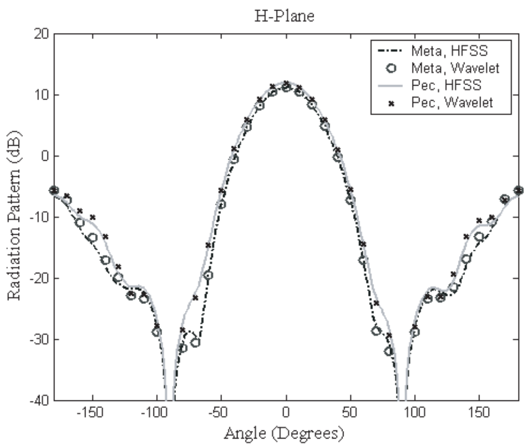

Figure 3: Radiation pattern H-Plane with and without metamaterial at frequency $F = 10$ GHz.

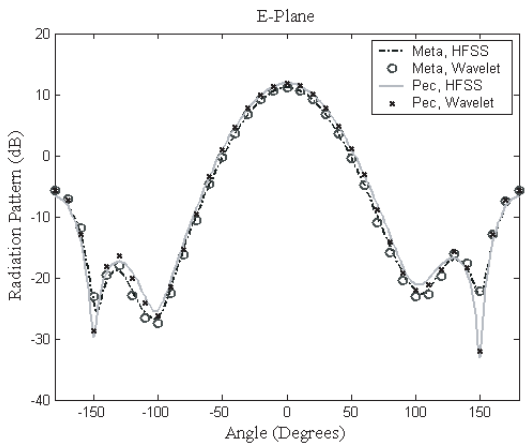

Figure 4: Radiation pattern E-Plane with and without metamaterial at frequency $F = 10$ GHz.

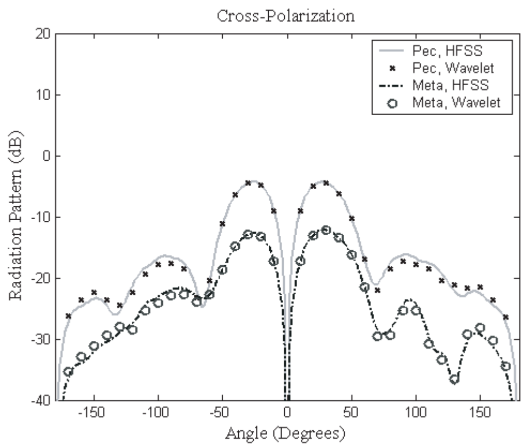

Figure 5: Cross polarisation radiation pattern, effect of the metamaterial, $\varepsilon_r = 0.5$, thickness $d = 1\,\text{mm}$, $F = 10\,\text{GHz}$.

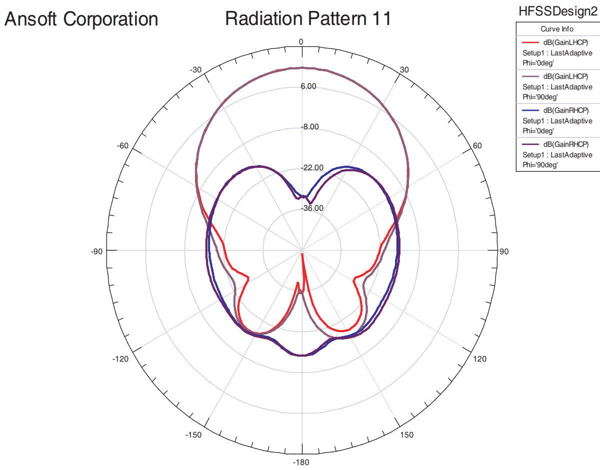

Figure 6: Radiation pattern without metamaterial at frequency $F = 10\,\text{GHz}$.

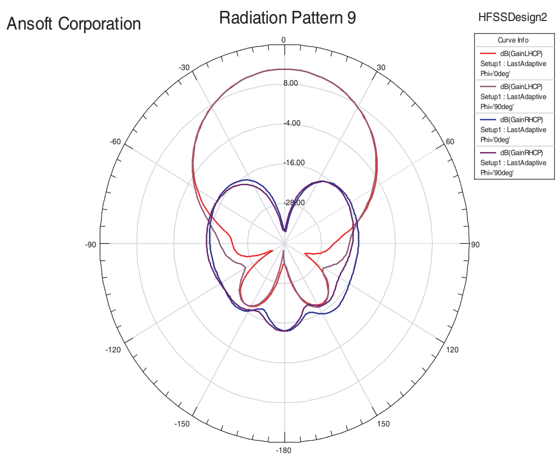

Figure 7: Radiation pattern with metamaterial at frequency $F = 10\,\text{GHz}$.

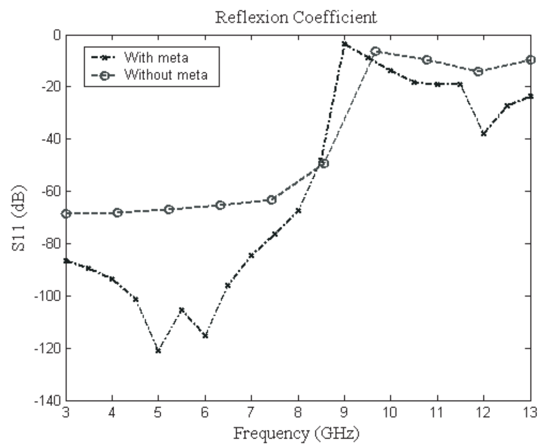

Figure 8: Reflection coefficient with and without metamaterial.

The reflection coefficient in Figure 8 shows a slight displacement of the bandwidth to the lower frequencies, from 9.6 GHz to 10 GHz, i.e., about 10%. This means that one can produce small antenna designs with a reduction in size of about 10%, or simply the bandwidth is enhanced of 10%.

4. CONCLUSIONS

A horn antenna for ultra-wide band (10–13 GHz) has been designed and tested using HFSS and compared to the moment method. The results obtained are in good agreement. The horn loaded with the metamaterial has shown a slight change in the radiation pattern and bandwidth of about 10%, but there is a remarkable effect on the directivity of the antenna. Some antenna miniaturisation is observed but the choice of metamaterial parameters could be further optimized in this respect.

REFERENCES

1. Akyurtlu, A. and D. H. Werner, "A novel dispersive FDTD formulation for modeling transient propagation in chiral metamaterials," *IEEE Transactions on Antennas and Propagation*, Vol. 52, No. 9, 2267–2276, September 2004.
2. Engheta, N., "An idea for thin subwavelength cavity resonators using metamaterials with negative permittivity and permeability," *IEEE Antennas and Wireless Propagation Letters*, Vol. 1, 10–13, 2002.

3. Erentok, A. and R. W. Ziolkowski, "Two-dimensional efficient metamaterial-inspired electrically-small antenna," *Microwave and Optical Technology Letters*, Vol. 49, No. 7, July 2007.
4. Zhu, F.-M. and J. Hu, "Improved patch antenna performance by using a metamaterial cover," *Journal of Zhejiang University Science A*, Vol. 8, No. 2, 192–196, 2007.
5. Wang, Y.-S., M.-F. Hsu, and S.-J. Chung, "A compact slot antenna utilizing a right/left-handed transmission line feed," *IEEE Transactions on Antennas and Propagation*, Vol. 56, No. 03, 675–683, March 2008.
6. Wu, B.-I., W. Wang, J. Pacheco, X. Chen, T. Grzegorczyk, and J. A. Kong, "A study of using metamaterials as antenna substrate to enhance gain," *Progress In Electromagnetics Research*, Vol. 51, 295–328, 2005.
7. Lier, E., "Review of soft and hard horn antennas, including metamaterial-based hybrid-mode horns," *IEEE Antennas and Propagation Magazine*, Vol. 52, No. 2, April 2010.
8. Hui, W. W. G., J. M. Bell, M. F. Iskander, and J. J. Lee, "Low-cost microstrip-line-based ferrite phase shifter design for phased array antenna applications," *IEEE Antennas and Wireless Propagation Letters*, Vol. 6, 86–89, 2007.
9. Ikram, S. and G. ahmad, "Design & implementation of a standard gain horn antenna for optimized gain and radiation pattern using mathCAD & HFSS," *Second International Conference on Electrical Engineering*, University of Engineering and Technology, Lahore, Pakistan, March 25–26, 2008.
10. Luo, G. Q., W. Hong, H. J. Tang, J. X. Chen, X. X. Yin, Z. Q. Kuai, and K. Wu, "Filtenna consisting of horn antenna and substrate integrated waveguide cavity FSS," *IEEE Transactions on Antennas and Propagation*, Vol. 55, No. 1, 92–98, January 2007.
11. Lee, K.-H., C.-C. Chen, and R. Lee, "UWB dual-linear polarization dielectric horn antennas as reflector feeds," *IEEE Transactions on Antennas and Propagation*, Vol. 55, No. 3, 798–804, March 2007.
12. Shafai, L., S. K. Sharma, B. Balaji, A. Damini, and G. Haslam, "Multiple phase center performance of reflector antennas using a dual mode horn," *IEEE Transactions on Antennas and Propagation*, Vol. 54, No. 11, 3407–3417. November 2006.
13. Yin, X.-C., C.-L. Ruan, S.-G. Mo, C.-Y. Ding, and J.-H. Chu, "A compact ultra-wideband microstrip antenna with multipole notches," *Progress In Electromagnetics Research*, Vol. 84, 321–332, 2008.
14. Venkatarayalu, N. V., C.-C. Chen, F. L. Teixeira, and R. Lee, "Numerical modeling of ultrawide-band dielectric horn antennas using FDTD," *IEEE Transactions on Antennas and Propagation*, Vol. 52, No. 5, 1318–1323, May 2004.
15. Lier, E. and A. Kishk, "A new class of dielectric-loaded hybrid-mode horn antennas with selective gain: Design and analysis by single mode model and method of moments," *IEEE Transactions on Antennas and Propagation*, Vol. 53, No. 1, January 2005.
16. Diamantis, S. G., A. P. Orfanidis, and G. A. Kyriacou, "Conical horn antennas employing an offset moment method and mode matching technique," *IEEE Transactions on Magnetics*, Vol. 45, No. 3, 1092–1095, March 2009.